Journal of Ocean, Mechanical and Aerospace
-Science and Engineering-, Vol.11

September 20, 2014

A Chebyshev Polynomial on Torque and Thrust Coefficients of Mathematical Propeller Properties for a LNG Manoeuvring Simulation

Sunarsih,[a], Agoes Priyanto,[a, b,*], Mohd. Zamani,[a], and Nur Izzudin,[a]

[a)] *Faculty of Mechanical Engineering, Unversiti Teknologi Malaysia, UTM Skudai 81300, Johor Bahru, Malaysia*
[b)]*Marine Technology Centre, Unversiti Teknologi Malaysia, UTM Skudai 81300, Johor Bahru, Malaysia*

*Corresponding author: agoes@fkm.utm.my

Paper History

Received: 15-September-2014
Received in revised form: 17- September -2013
Accepted: 19- September -2014

ABSTRACT

The estimated torque and thrust coefficients in four quadrants of marine propeller in a LNG manoeuvre control system is essential for the total performance of the vessel. A Chebyshev n-order polynomial that approximated a continuous function over the interval advance speed J [-1, 1] to calculate the torque and thrust coefficients as well as the shaft speed, is utilized to get the propeller properties. The Dynamical modeling and simulation of the marine propeller across the four quadrants are schemed and applied to the marine propeller B-4.58. The results are compared with both open water experiments and open water numerical tests using ANSYS-Fluent. The comparisons show that the chebyshev polynomial agreed well with both experiments and numerical tests and deduce that the polynomial provides a new practically approach estimation on torque and thrust coefficients in four quadrants of marine propeller for the vessel operations. Then the polynomial coefficients from Chebyshev n-order polynomial were used to express the mathematical model for the propeller thrust and torque characteristics and applied in the manoeuvring simulation programming.

KEY WORDS: *Chebyshev Polynomial, Propeller Properties, Ansys Fluent, Manoeuvring Simulation*.

1.0 INTRODUCTION

There exist some notable problems regarding ship manoeuvring which has been observed to change significantly according to canal regions. The ship-bank effect in shallow water becomes significant when the ship travels close to the bank. A large vessel experiences lateral force and turning moment by asymmetric flow around the ship's hull due to the presence of the bank in a very narrow waterway [15], [16], [17]. This phenomenon may even become critical [18)] when as it causes difficulties in controlling the ship along its intended course this in turn increases the possibility of grounding or collision. In November 2007 at Suez Canal, the same type of ship had the same incident when the ship was turning back to the starboard. This point can be illustrated by two pilots and the master failed to regain control of the LNG vessel following a manoeuvre at reduced-speed in a canal. The vessel was proceeding South with new pilots and approached close to the Eastern bank, while navigating the canal bend opposite a Lake. The vessel appeared to become course-unstable after successive 35 degree helm operations to port and starboard, during which the vessel struck the Eastern bank 15 minutes after the start of the manoeuvre and grounded on the Western bank after a further 4 minutes. [18] have proposed valuable information on potential remedial actions for LNG tanker manoeuvre in the canal, such as a combination work between fitting two pairs of fins and increasing the effectiveness of the existing rudder at low ship speed and developed the manoeuvring simulation by MATLAB Simulink to solve the problem.

The manoeuvring simulation solves the surge, sway, and yaw motions with respect to CoG of tanker. The mathematical model of external forces on the tanker composed of hydrodynamic hull, rudder force and propeller force as well as the hydrodynamic hull-banks interactions. In the simulation the mathematical model propeller force in X-direction were expressed by polynomial

coefficients order three from *Kt-J*, and *Kq-J* diagrams. The polynomial coefficients expression for the propeller thrust and torque characteristic were determined from the open water propeller tests.

Such a model in curve from is immediate and obvious, but it is not convenient to do mathematical analysis and simulation programming. Usually polynomial fitting form is adopted by ordinary polynomial. The principle weakness of ordinary polynomial fitting is that the fitting results from open water tests are not in common use. For different order *n*, in order keep higher fitting accuracy, it is necessary to use different set of polynomial coefficients and to refit new. Using ordinary polynomial fitting to meet different requirements, many set of coefficients must be prepared and it is convenient. If polynomial coefficients are kept invariant, only the order number is increased and decreased. The best way this problem is to use Chebyshev polynomial fitting.

$$Kt = T/\left(\rho D^4 N^2\right), (N \neq 0) \quad (1)$$

$$Kq = Q/\left(\rho D^5 N^2\right), (N \neq 0) \quad (2)$$

$$J = v_p/(DN), (N \neq 0) \quad (3)$$

where v_p is the propeller velocity relative to water, T and Q are propeller thrust and torque respectively, D is propeller diameter. For a given propeller pitch to D ratio P/D, the relation T, Q and J are expressed as

$$Kt = K_t(J),\ Kq = K_q(J) \quad (4)$$

On K_t-J diagram or K_q-J diagram stride across four quadrants generally and Kt, Kq and J stretch to infinite. When N and v_p are not equal to zero at the same time they are defined as

$$K't = T/\left(\rho D^2\left(v_p{}^2 + D^2N^2\right)\right) = Kt/\left(1 + J^2\right) \quad (5)$$

$$K'q = Q/\left(\rho D^3\left(v_p{}^2 + D^2N^2\right)\right) = Kq/\left(1 + J^2\right) \quad (6)$$

$$J' = v_p/\sqrt{v_p^2 + D^2N^2} \quad (7)$$

It can be seen that J=(-∞,∞) is mapped to J=(-1,1).

This paper will discuss Chebyshev polynomial and get results the polynomial coefficients of the propeller B4-58, disc square ratio A_0/A_d =0.58, blade=4, wing type section and screw pitch ratio P/D=1. The results then were compared with both open water experiments and open water numerical tests using ANSYS-Fluent V.6. As an application, this method is applied in the mathematical model for propeller properties in Chebyshev polynomial and used to simulate manoeuvring of LNG tanker.

2.0 NUMERICAL ESTIMATION.

2.1. Chebyshev Polynomial

Propellers are usually designed to produce thrust in one direction and propel the ship ahead. Nonetheless, the ship sometimes has to produce thrust in the reverse direction to propel the ship backward. Furthermore, the propeller maybe uses to decelerate the ship by running in the opposite direction of the advance speed. Addressing these issues, the four quadrants of propeller operation provide discretion in serving such functions. The characteristics, as presented in Table 1, are determined by the positive or negative operation of ship speed (V_s) and the propeller rotation (N).

Table 1: Propeller quadrants of operation.

	1	**2**	**3**	**4**
N	≥ 0	< 0	< 0	≥ 0
V_s	≥ 0	≥ 0	< 0	< 0

where V_p is advance speed of the propeller relative to water approximated using the following expression: The thrust coefficient Kt, torque co

$$V_p = (1\text{-}w)\ V_s \quad (8)$$

The standard (first quadrant) and four-quadrant propeller characteristics used to describe the thrust and torque in steady-state conditions. However, the degradation of the propeller performance will occur if the propeller is subjected to cross-flow or is not deeply submerged by employing thrust and torque loss functions. In that case, additional measurements of the cross flow velocity and the propeller submergence are necessitated. The following Fig. 1 illustrates the four quadrants representing the four combinations of speed and thrust directions.

When the ship manoeuvres in steady state, the advance ratio J varies in a small range ($J \in [0.6, 0.8]$) while it significantly changes during the dynamic state and even can be negative in values [1] – [10]. Usually polynomial fitting form is adopted as follows:

$$g(x) = \sum_{j=0}^{n} b_j x^j = b_0 + b_1 x + \ldots + b_n x^n \quad (9)$$

Meanwhile a continuous function over the interval [-1, 1] can be expressed also approximately as n-th order of Chebyshev polynomial [5] written as:

$$f(x) = \sum_{j=1}^{n} a_j T_j(x) \quad (10)$$

where $T_0(x)=1$, $T_1(x)=x$, $T_2(x)=2x^2 - 1$, $T_3(x)=4x^3 - 3x$, … while the general recursive formula for $T_k(x)$ is given by:

$$T_k(x) = 2xT_{k-1}(x) - T_{k-2}(x);\ k \geq 2 \quad (11)$$

The feature of the Chebyshev polynomial is that $T_i(x)$ and $T_k(x)$ are orthogonal to each other and the polynomial coefficients are independent of the order n. Furthermore, the fitting error is small and the fitting result with finite order n is the best approximation within the meaning of minimum square error. It is convenient to change into ordinary polynomial a given Chebyshev polynomial expression.

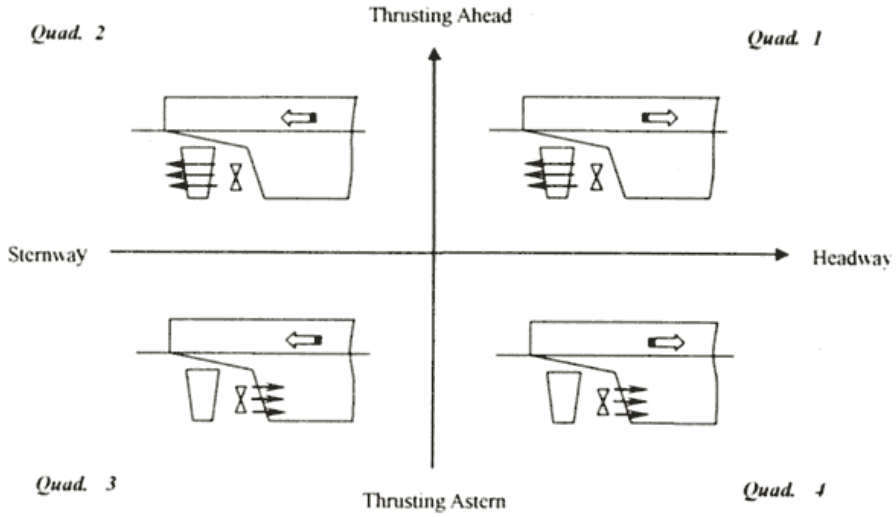

Figure 1: Four quadrants of ship speed and propeller operations.

For a given screw-pitch ratio *H/D*, the approximation of the propeller thrust coefficient K_t and torque coefficient K_q properties across four quadrants with such Chebyshev polynomial (n=8) are expressed by:

$$Kt'(J') = \frac{1}{2}a_{0t}T_0(J') + a_{1t}T_1(J') + \cdots + a_{nt}T_n(J') \quad (12)$$

$$Kq'(J') = \frac{1}{2}a_{0q}T_0(J') + a_{1q}T_1(J') + \cdots + a_{nq}T_n(J') \quad (13)$$

Substituting Chebyshev polynomial $a_0 - a_n$ in Table 2 into extending $T_0 - T_n$, by definition. Moreover the ordinary polynomials are expressed by:

$$Kt'(J') = b_0 + b_{1t}J + \cdots + b_{nt}J^n \quad (14)$$

$$Kq(J') = b_0 + b_{1q}J + \cdots + b_{nq}J^n \quad (15)$$

The ordinary polynomial and its coefficients $b_0 - b_n$ can be obtained as shown in Table 3 by using Eqs.(12) – (15).

Table 2: Chebyshev Polynomial Coefficients of Thrust and Torque Properties.

a	Kt'		Kq'	
	n>0	n<0	n>0	n<0
a_0	0.3888	-0.2641	0.05315	-0.04467
a_1	-0.2338	-0.2274	-0.03093	-0.03423
a_2	-0.1664	0.1254	-0.0226	0.0249
a_3	-0.02003	-0.02646	-0.00406	-0.00458
a_4	0.00134	-0.00152	0.000832	-0.00154
a_5	0.05241	0.04883	0.006672	0.007792
a_6	-0.02842	0.02704	-0.00184	0.004162
a_7	0.02029	0.01888	0.004078	0.004694
a_8	0.01766	-0.00632	0.002371	-0.001650

Table 3: Ordinary Polynomial Coefficients of Thrust and Torque Properties

b	Kt		Kq	
	n>0	n<0	n>0	n<0
b_0	0.04924	-0.04312	0.1944	-0.13205
b_1	0.03224	0.03609	0.21042	0.20466
b_2	-0.02510	0.027739	-0.10317	0.077748
b_3	0.00118	0.001799	0.004326	0.005715
b_4	0.00009	-0.00041	-0.00031	0.000352
b_5	0.00452	0.005294	0.033132	0.030868
b_6	0.05450	-0.00696	0.025768	-0.02452
b_7	0.00389	0.00431	0.020288	0.018878
b_8	0.01766	-0.0006	-0.01577	0.005644

The LNG's propeller has been taken to describe the method of calculating the alternatives properties, Chebyshev polynomial with n=8 were used. By calculation, we select screw pitch ratio *P/D*=1.0. Substituting into Eqs(12) – (15) the resulting expressions for interpolation for thrust coefficient and torque coefficients are plotted in Figs.(2) – (3).

2.2. Computational fluid dynamic (CFD).

The computational fluid dynamics, as known as the CFD has become a practical tool in the simulation of hydrodynamics of marine devices, especially propeller [11] – [14]. A CFD study on the propeller open water test using the stationary domain length of about 6-7 times the propeller diameter to simulate the flow source and sink was conducted. The rotational domain which was close proximity to the propeller, could give a good simulation for the rotating region of fluid adaption surrounding the propeller. It adopted the multiple reference frame method, and the bigger rotating part was selected and it would produce more accurate results. A four bladed propeller B4-58 screw pitch ratio *P/D*=1.0 was used in the propeller properties estimation. The following assumptions or approach are implemented, namely the fluid domain numerically modelled via a finite volume method based

on the Reynold-Average Navier Stokes (RANS) equations, and the accuracy for applicability of first quadrant steady flow as shown in Fig. 1 were compared with the Chebyshev polynomial and the experimental results

In Cartesian tensor form the general RANS equations for continuity fluid can be written as:

$$\frac{\partial \rho}{\partial t}+\frac{\partial(\rho u_i)}{\partial x}=0 \tag{16}$$

The momentum equation becomes:

$$\frac{\partial(\rho u_i)}{\partial t}+\frac{\partial(\rho u_i u_j)}{\partial x_j}=-\frac{\partial p}{\partial x_i}+\frac{\partial}{\partial x_j}\left[\mu\left(\frac{\partial u_i}{\partial x_j}+\frac{\partial u_j}{\partial x_i}-\frac{2}{3}\delta_{ij}\frac{\partial u_i}{\partial x_i}\right)\right]+\frac{\partial}{\partial x_j}\left(-\rho\overline{u_i}'\overline{u}_j'\right) \tag{17}$$

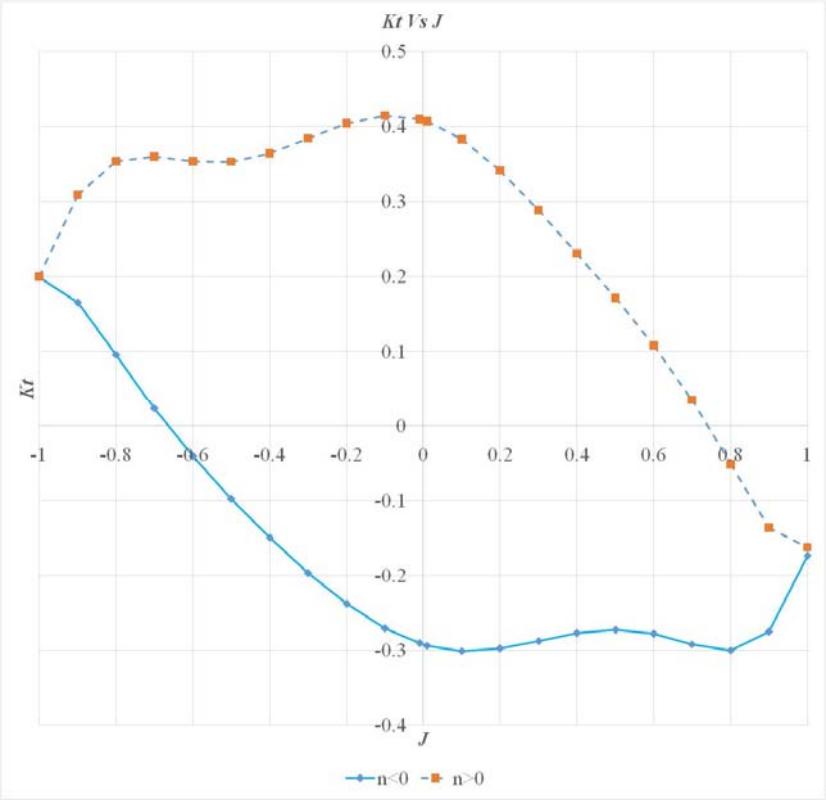

Figure 2: Thrust coefficient across four quadrants.

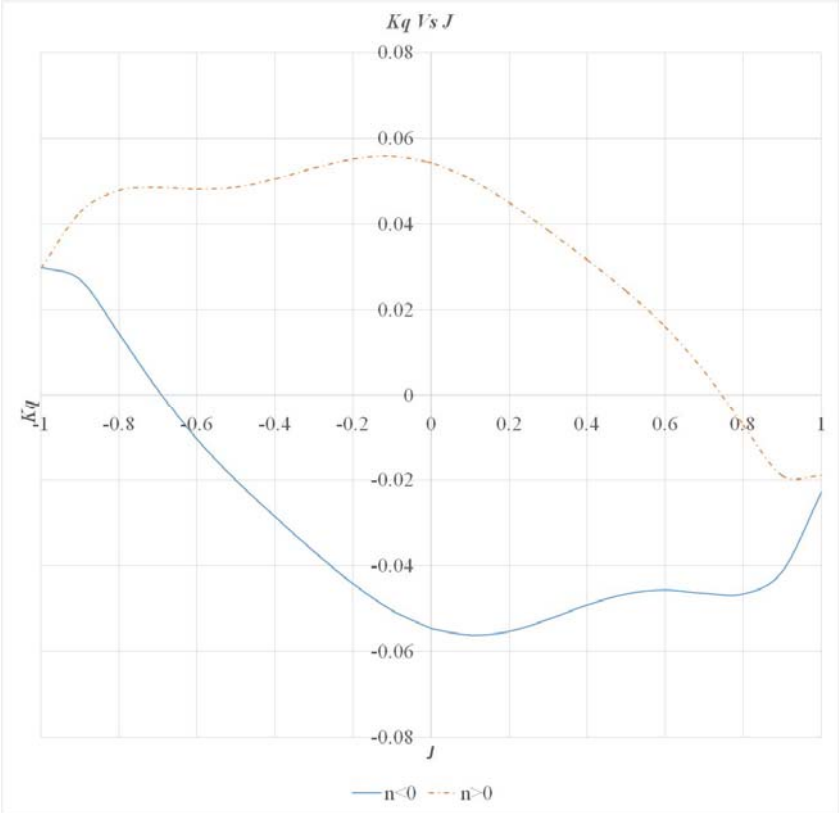

Figure 3. Torque coefficient across four quadrants.

where δij in the Eq. (17) is the Kronecker delta, $(-\rho\overline{u_i'u_j'})$ are the unknown Reynolds stresses that have to be modelled to close the momentum equation. With Boussinesq's eddy-viscosity assumption and two transport equations for solving a turbulence velocity and turbulence time scale (turbulence modelling), RANS equations are closed. The commercial software Ansys Fluent applied a cell-centred finite volume method, and the velocity in the RANS equations in Eqs. (16) and (17) are solved in both moving reference frame for the steady calculation and the moving mesh for the transient calculation.

To model the turbulent flow, the steady turbulent model was applied in the ANSYS Fluent which is the standard k-epsilon model for the simulation. In the simulation, the propeller type B 4 – 58 was meshed as shown in Fig. 3. For the computational domain as shown in Fig. 4, the propeller blades were mounted on two finite long constant radius cylinders. The two types of cylinder domains, which have been developed, were stator domain and rotor domain. For the stator domain, the inlet flow is *Lsi* = 2*D* from blade, the outlet flow at *Lso*= 6*D* and the outer boundary is *Ds*=3.6*D*. While the rotor domain, the upstream remained *Lbr*=0.2D but the downstream was extended for cases open water test between *Lfr*= 0.4D and 0.7D, and the outer boundary is 1.4D. The turbulent model was simulated in the rotor domain by using the stator-rotor approaches such as the multiple reference frame (MRF) and the sliding mesh (SM) method. These computational configurations are distinguished mainly by its size of rotational domain's open water tests.

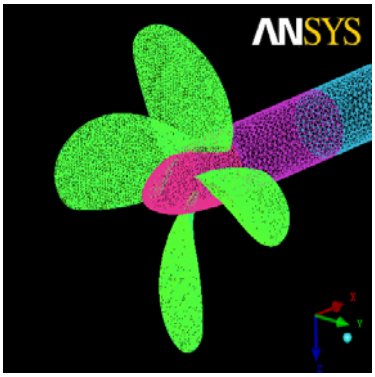

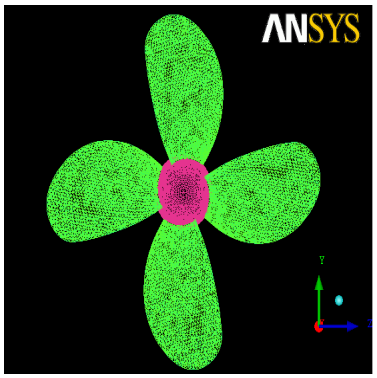

Figure 3: Propeller meshing.

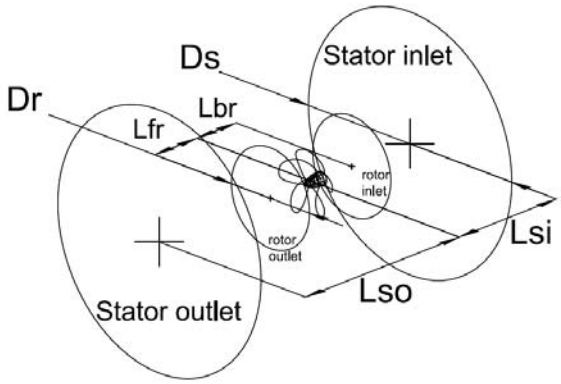

Figure 4: Computational domain for the propeller.

An advance speed (u_a) is used to initiate the inlet flow. Detailing the boundary conditions, velocity inlet was selected for stator inlet plane with intensity and viscosity ratio of 10 for the turbulent specification method. Pressure outlet is defined for the stator outlet with zero gauge pressure and similar turbulent specification as stator inlet. Convergence criterion was set up to 10^{-3} and solutions were converged within ranges of 200 to 1200 iterations as shown in Fig. 5, but not for very high J values. The open water curves is simulated by varying propeller rotation rate and fixed the value of advance speed. Convergence was set to 0.001 and iteration was converged to mere 600 in average open water condition. The rotating range between n=50 to 190 rpm were assigned and all boundaries inside this domain was specified as adjacent to cell zone, or the rotational fluid zone.

3.0 OPEN WATER TESTS.

The tests were carried out at the Marine Technology Centre, Universiti Teknologi Malaysia. The basin, 120 m long, 4 m wide and 2.5 m deep is equipped with a towing carriage that can reach a masximum speed of 4 m/s with a wave generator able to generate waves up to 0.4 m. We employed a three phase brushless motor in combination with a drive equipped with a built-in torque controller and a build-in shaft speed controller. In this way we could choose to control the motor torque in order to obtain the desired motor torque or the shaft speed to obtain the desired ω. The motor was connected to the propeller shaft through a gear-box with ratio 1:1. The rig with motor, underwater housing, shaft and propeller was attached to the towing carriage in order to move the propeller through the water. The tests were performed on a fixed pitch propeller B4-58.

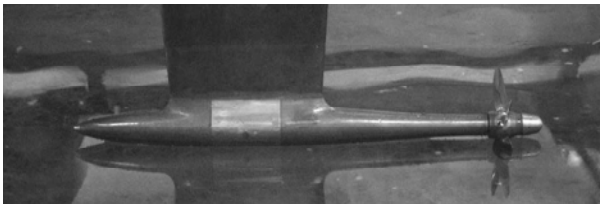

Figure 5: Open Water tests.

The shaft speed was measured on the motor shaft with a tachometer dynamo. The thrust and torque were measured with an inductive transducer and a strain gauge transducer placed on the propeller shaft, respectively. The measurement of the motor torque was furnished by the motor drive. A picture of the propeller system is presented in Fig. 5.

4.0 RESULTS AND DISCUSSION.

In this section, it isn't difficult to get an ordinary propeller atlas for the first quadrant. If alternatives properties with higher accuracy can be compared and found on the first quadrant by using other methods, it will be significant.

As an application this method is used to calculate LNG's propeller's alternative properties in Chebeyshev polynomial form providing in preceding section. Then they are used in comparison with calculation results of LNG's propeller from Ansys FLUENT and Open Water tests. The model lays a foundation for LNG manoeuvering simulation. CFD of Ansys FLUENT and open water experiments practice shows that the results are very close to the practical data, as shown in Figs. 5 and 6, therefore are effective.

The Figs 6 and 7 displays the thrust and torque coefficients which decrease simultaneously with respect to the increase of advance ratio J values. A slight difference appears at both end points of comparison between the Chebyshev polysnomial and the experiment result. At the point of J = 0.4, the characteristic of the trust and torques coefficients are approaching similarly which values to 0.20 for Kt and 0.285 for $10Kq$. However, the trend is quite lower for the estimation generated from the ANSYS Fluent. The results reveal that the torque coefficients generated from the Chebyshev expression for the inside domain have a fairly similar trend and values with the experimental result and also agreed well with the previous CFD study which adopted the multiple reference frame (MRF) method, that the bigger rotating part (Lr) is used and will produce more accurate results.

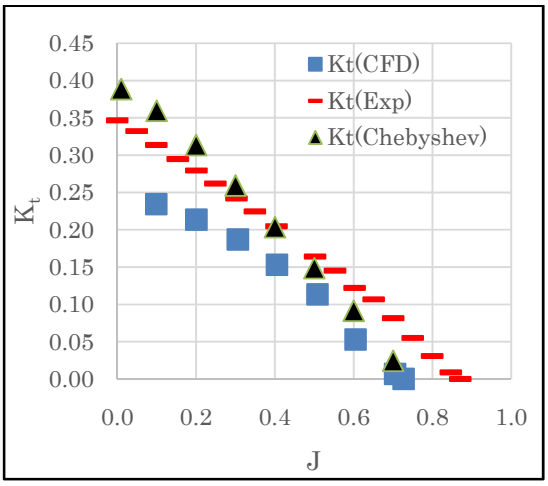

Figure 6: Comparison results for thrust coefficients.

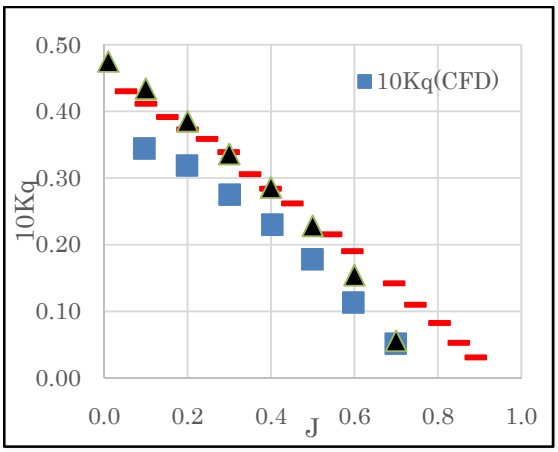

Figure 7: Comparison results for torque coefficients.

5.0 LNG'S MANOEUVRING SIMULATION.

The mathematical model can be described by the Eqs. (18) – (20), using the coordinate system in Figure 8. As shown in Figure 7, (U) is the actual ship velocity that can be decomposed in an advance velocity (u) and a transversal velocity (v). The LNG ship has also a rotation velocity (r) with respect to the z-axis. This axis is normal to the XY plane and passes through the LNG ship centre of gravity (C.G). (β) is the angle between U and the x-axis and it is called drift angle. (ψ) is the LNG ship heading angle and (δ) is the rudder angle. X , Y and N represents the hydrodynamic force and moment acting on the mid ship of hull.

$$X = m(\dot{u} - rv) \tag{18}$$

$$Y = m(\dot{v} + ru) \tag{19}$$

$$N = I_{zz}\dot{r} \tag{20}$$

Eqs. (18), (19), and (20) correspond to the surge, sway, and yaw motions, respectively. m is the mass of the ship, I_{zz} is the moment of inertia with respect to the z-axis. u , v, and r are the surge, sway, and yaw velocities and $\dot{u}$, $\dot{v}$, and $\dot{r}$ are the surge, sway, and yaw accelerations, respectively. X and Y represent the forces acting in the X and Y directions whilst N is the moment with respect to the z-axis. These forces and moment can be described by separating them into the following components:

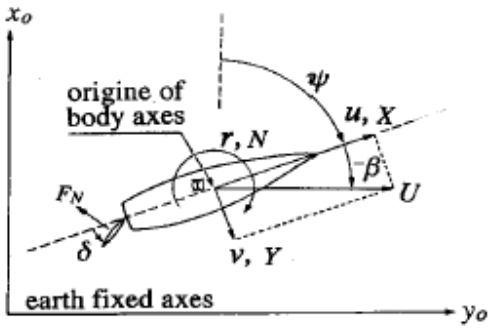

Figure 8: Comparison results for torque coefficients.

$$X = X_H + X_P + X_R \tag{21}$$

$$Y = Y_H + Y_P + Y_R + Y_{BK} \tag{22}$$

$$N = N_H + N_P + N_R + N_{BK} \tag{23}$$

Where: the subscripts *H, P, R* and *BK* refer to hull, propeller, rudder and bank effect, respectively. Eqs. (4), (5) and (6) follow to the concept given by the Mathematical Modelling Group (MMG) of Japan [Ogawa, A and Kansai, H , 1987]. The forces and moments acting on the hull can be approximated by the following polynomials of v' and r' by the following expressions

$$X_H = \frac{1}{2}\rho L^2 U^2 \left[X'_{\dot{u}}\dot{u}' + X'_{vr}v'r' + X'_{vv}v'^2 + X'_{rr}r'^2\right] + \frac{1}{2}\rho L^2 U^2 R'_{TM} \tag{24}$$

$$Y_H = \frac{1}{2}\rho L^2 U^2 \left[\begin{array}{r} Y'_{\dot{v}}\dot{v}' + Y'_{\dot{r}}\dot{r}' + Y'_v v' + Y'_r r' + Y'_{vvv}v'^3 + \\ Y'_{vvr}v'^2 r' + Y'_{vrr}v'r'^2 + Y'_{rrr}r'^3 \end{array}\right] \tag{25}$$

$$N_H = \frac{1}{2}\rho L^3 U^2 \left[\begin{array}{r} N'_{\dot{v}}\dot{v} + N'_{\dot{r}}\dot{r}' + N'_v v' + N'_r r' + \\ N'_{vvv}v'^3 + N'_{vvr}v'^2 r' + N'_{vrr}v'r'^2 + N'_{rrr}r'^3 \end{array}\right] \tag{26}$$

The primes in Eqs. (24) – (26) refer to the non-dimensional quantities, defined as the following:

$$v' = \frac{v}{U};\quad \dot{v}' = \frac{\dot{v}L}{U^2};\quad r' = \frac{rL}{U};\quad \dot{r}' = \frac{\dot{r}L^2}{U^2}$$

$$X' = \frac{X}{\frac{\rho}{2}L^2U^2};\quad Y' = \frac{Y}{\frac{\rho}{2}L^2U^2};\quad N' = \frac{N}{\frac{\rho}{2}L^3U^2}$$

$$R'_{TM} = \frac{R}{\frac{\rho}{2}L^2U^2} \tag{27}$$

The mathematical force and moment of propeller X_P, Y_P, N_P are expressed as the following.

$$X_P = (1-t_P)\rho K_T D_P^4 n^2$$
$$Y_P = 0 \tag{28}$$
$$N_P = 0$$

$$X'_P = \frac{X_P}{\frac{1}{2}\rho L^2U^2} \tag{29}$$

Where for a given screw-pitch ratio H/D, the approximation of the propeller thrust coefficient K_t and torque coefficient K_q properties across four quadrants with such Chebyshev polynomial (n=8) are expressed by substituting Chebyshev polynomial $a_0 - a_n$ from Table 2 into extending $T_0 - T_n$, by definition. Moreover the ordinary polynomials are expressed by Eqs. (14) and (15) and its coefficients $b_0 - b_n$ can be obtained from Table 3. Here t_p, n, D_P, w_P, J_P, *and* $b_0 - b_n$ are thrust deduction factor, ordinary polynomial coefficient in straight forward moving (first quadrant), propeller revolution, propeller diameter, effective wake fraction coefficient at propeller location.

Comparison between simulated and free running results was illustrated in Figures 8 and 9. Zig-zag manouevre for 10° and 20° rudder angle and turning manouevre for a 35° rudder angle are shown in Figures 8 and 9, respectively. Generally speaking, the trends of free running tests in 35° rudder angle turning manoeuvre; and zig-zag manoeuvre for 10° and 20° rudder angle were quite similar to those of the simulation results.

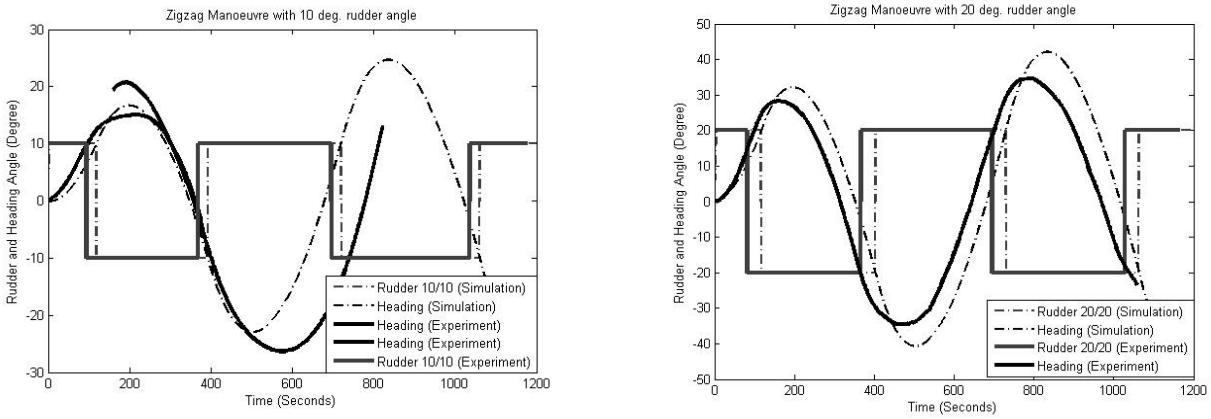

Figure 9: Comparison zig-zag manouevre with 10^0 and 20^0 rudder angle between Simulation and Free Running

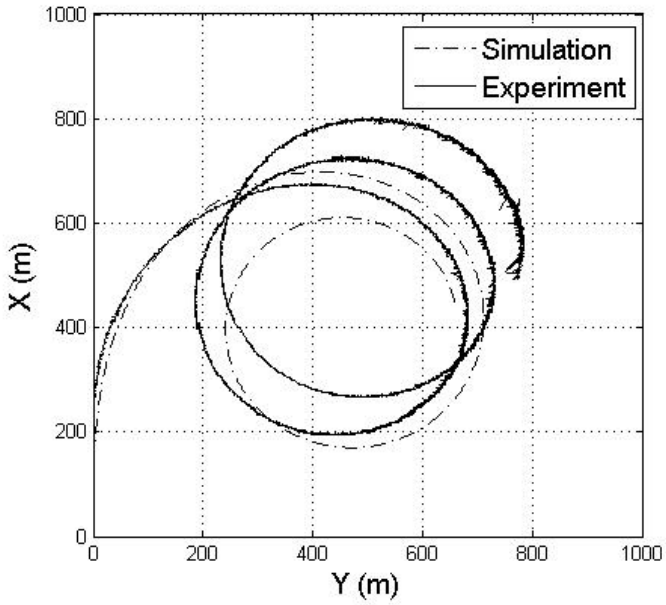

Figure 10: Turning manouevre with rudder angle of 35^0 of Simulation and Free Running for ship

5.0 CONCLUSION

1. A Chebyshev fitting way for propeller is discussed. As a example, Chebyshev fitting results for Table 1 are given.
2. As an application example, an alternative propeller property of LNG for first quadrant is compared with the CFD and Open Water Tests, and a simulation mathematical model of first quadrant properties for the LNG's Manoeuvring simulation. The results are very close among them, and very close to the practical simulation data.
3. For LNG's manoeuvring simulation in the Canal, a model across four quadrants for the LNG and a propulsion system model for LNG across four quadrants are required to be set up. Then they will be used in safely simulation in a Canal of LNG;s forward and backward movement

ACKNOWLEDGEMENTS

The authors would like to thank and acknowledge financial support from UniversitiTeknologi Malaysia and Ministry of Higher Education through the Tier 1 Research University Grant Vot No 04H2.

REFERENCE

1. Pivano, L., Johansen, T. A., &Smogeli, o. N. (2009). A four-quadrant thrust estimation scheme for marine propellers: Theory and experiments. *IEEE Transactions on Control Systems Technology, 17*(1), 215.
2. Li, R., Zhang, W. X., & Li, H. Y. (2012). Modeling and Simulation of Propeller and Hull System for Marine Propulsion Plant. *Advanced Materials Research, 383*, 2121-2125.
3. Mitja Morgut, E. N. (2009). "Comparison of Hexa-Structured and Hybrid-Unstructured Meshing Approaches for Numerical Prediction of the Flow Around Marine Propellers." First International Symposium on Marine Propulsors smp'09, Trondheim, Norway: 7.
4. Jan Kulczyk, L. S., Maciej Zawiślak (2007). "Analysis Of Screw Propeller 4119 Using The Fluent System." Archives Of Civil And Mechanical Engineering 7(4): 9.
5. Chi, H.-h., & Li, D.-p. (2006). Application of Chebyshev polynomial to simulated modeling. *Journal of Marine Science and Application, 5*(4), 38-41.
6. Jiang, p., Yao, Y., & Fan, S. (2011, 15-17 April 2011). *Simulation for the propeller loading of marine electrical propulsion based on matlab.* Paper presented at the Electric Information and Control Engineering (ICEICE), 2011 International Conference on.
7. Ye, B., Wang, Q., Wan, J., Peng, Y., & Xiong, J. (2012). A Four-Quadrant Thrust Estimation Scheme Based on Chebyshev Fit and Experiment of Ship Model. *Open Mechanical Engineering Journal, 6*(2), 148-154.
8. Kim, J., & Chung, W. K. (2006). Accurate and practical thruster modeling for underwater vehicles. *Ocean Engineering, 33*(5), 566-586.
9. Pivano, L., Fossen, T. I., & Johansen, T. A. (2006). *Nonlinear model identification of a marine propeller over four-quadrant operations.* Paper presented at the the 14th IFAC Symp. Syst. Identification (SYSID).
10. Lehn, E. (1992). FPS-2000 mooring and positioning, part 1.6 dynamic positioning—thruster efficiency: Practical methods

for estimation of thrust losses: Technical Report 513003.00. 06. Marintek, SINTEF, Trondheim, Norway.
11. Seo, J. H., Seol,D.M. ,Lee,J.H., Rhee,S.H. (2010). Flexible CFD meshing strategy for prediction of ship resistance and propulsion performance. *Inter J Nav Archit Oc Engng,* 2**,** 139-145.
12. Zadravec, S. B., M. Hribersek (2007). The Influence of Rotating Domain Size of in a Rotating Frame of Reference Approach for Simuation of Rotating Impeller in a Mixing Vessel. *Journal of Engineering Science and Technology,* 2**,** 126-138.
13. Paik, B.G., Kim, G.D., Kim, K.S., Kim, K.Y., Suh, S.B. (2012). Measurements of the rudder inflow affecting the rudder cavitation. *Ocean Engineering,* 48**,** 1-9.
14. W.P.A. van Lammeren, J.D. van Manen, M.W.C. Oosterveld. (1969). The Wageningen B-screw series, *Trans. SNAME*, 77, pp. 269–317.
15. Fujino, M., 1968, "Experimental studies on ship manoeuvrability in restricted waters-Part 1", International Shipbuilding Progress, Vol.15, No.168, pp.279-301.
16. Duffy, J.T, 2002. Prediction of bank induced sway force and yaw moment for ship handling simulator. Ship Hydrodynamics Centre, Australian Maritime College (AMC).
17. PIANC, 1992. Capability of ship manoeuvring simulation models for approach channels and fairways in harbours. Report of Working Group no. 20 of Permanent Technical Committee II, Supplement to PIANC Bulletin No. 77, pp. 49
18. Maimun, A, Priyanto, A, et. al (2013). A mathematical model on manoeuvrability of a LNG tanker in vicinity of bank in restricted water, Safety Science 53**,** 34-44.